

Self-Assembly of Microtubules and Molecular Motors: Interaction of Polar Rods

Igor Aronson

Argonne National Laboratory

with

Lev Tsimring,

University of California, San Diego

Phys Rev E **71** 050901(R) 2005



Supported by the U.S. Department of Energy

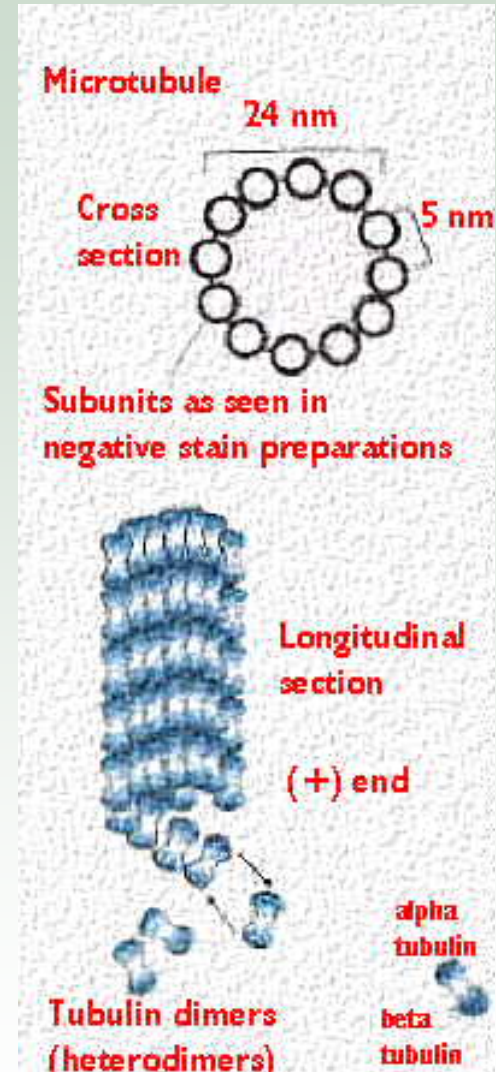
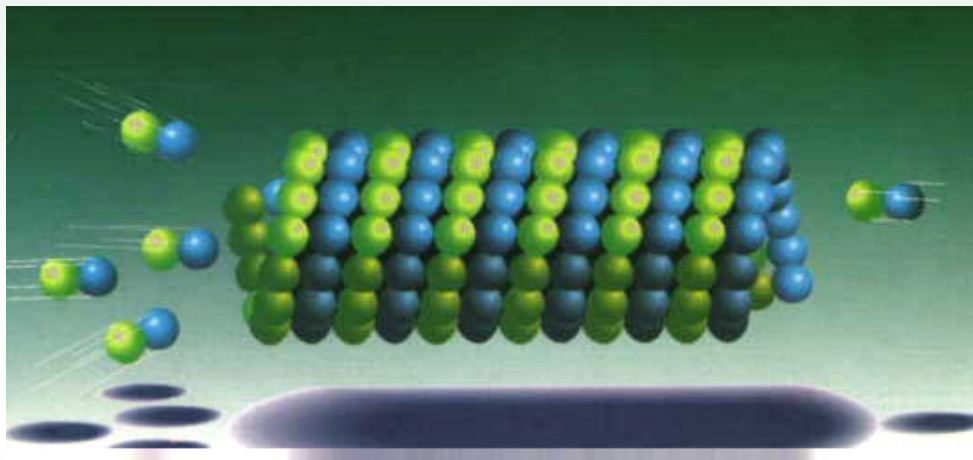
Outline

- Introduction
- *in-vitro* experiments
- Review of recent theories
- Maxwell model for polar rods and granular analogy
- Aster and vortices
- Conclusion
- New systems



Microtubules

- Very long rigid polar hollow rods (length – 5-20 microns, diameter -40 nm, Persistent length – few mm)
- Length varies in time due to polymerization/depolymerization of tubulin
- Multiple function in the cell machinery: cytoskeleton formation, cell division, cell functioning



Molecular motors-Associated Proteins

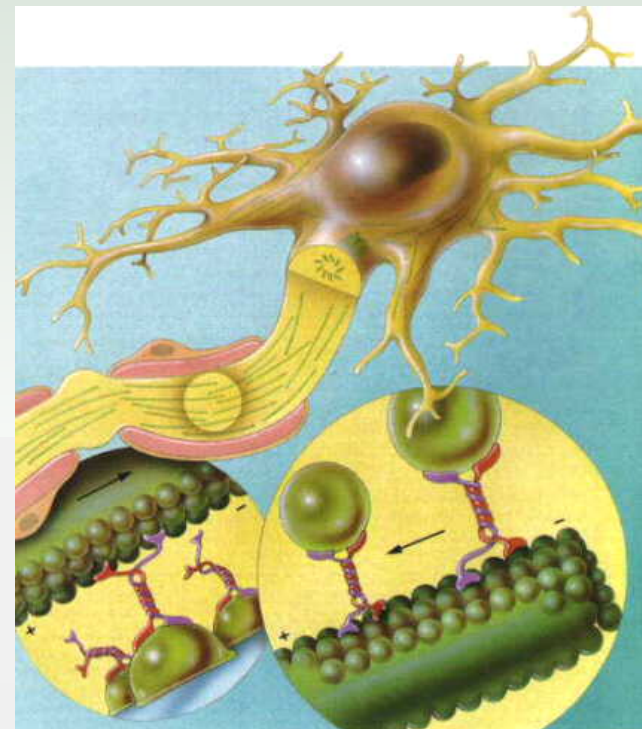
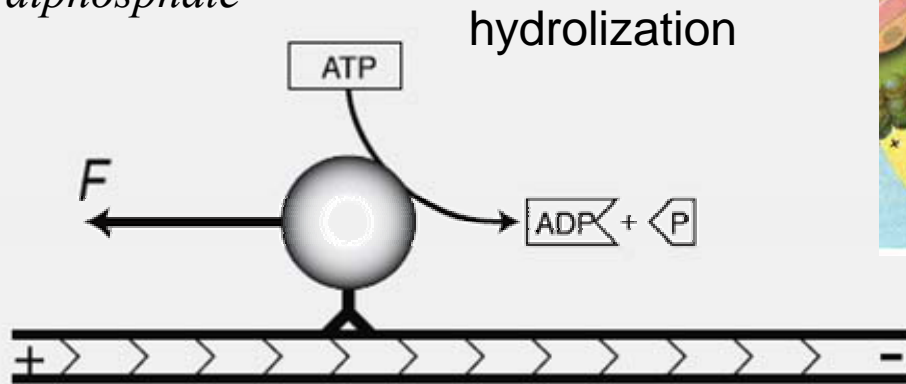
- **Linear motors** (kinesin, dynein, myosin) cytoskeleton formation, transport
- **Rotary motors:** (flagellar motor, F-ATPase) flagella rotation, ATP synthesis
- **Nucleic acid motors:** (helicase, topoisomerase) – DNA unwinding/translocation

Linear motors:

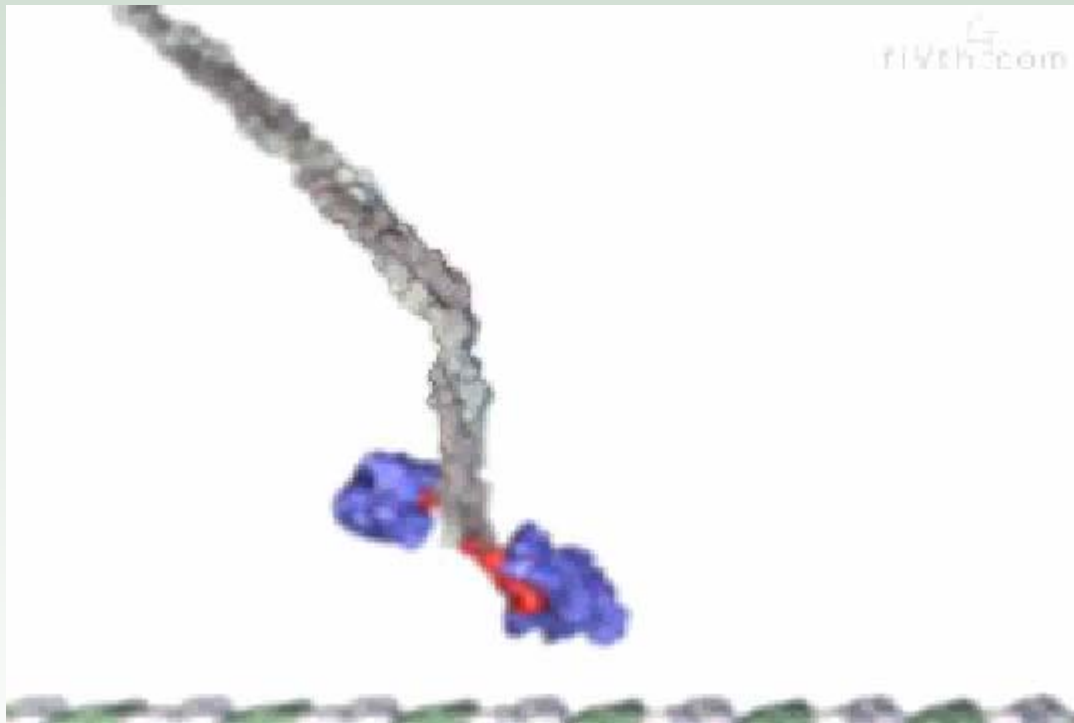
- Have one or two ‘heads’
 - One attached to MT
 - Other attached to vesicles, granules, or another MT
- Take energy from hydrolysis of ATP
- Speed $\sim 1\mu\text{m/s}$, step length 8 nm, run length $\sim 1\mu\text{m}$
- Exert force about 6 pN

ATP – Adenosine triphosphate

ADP- Adenosine diphosphate



Simulations of MM motion

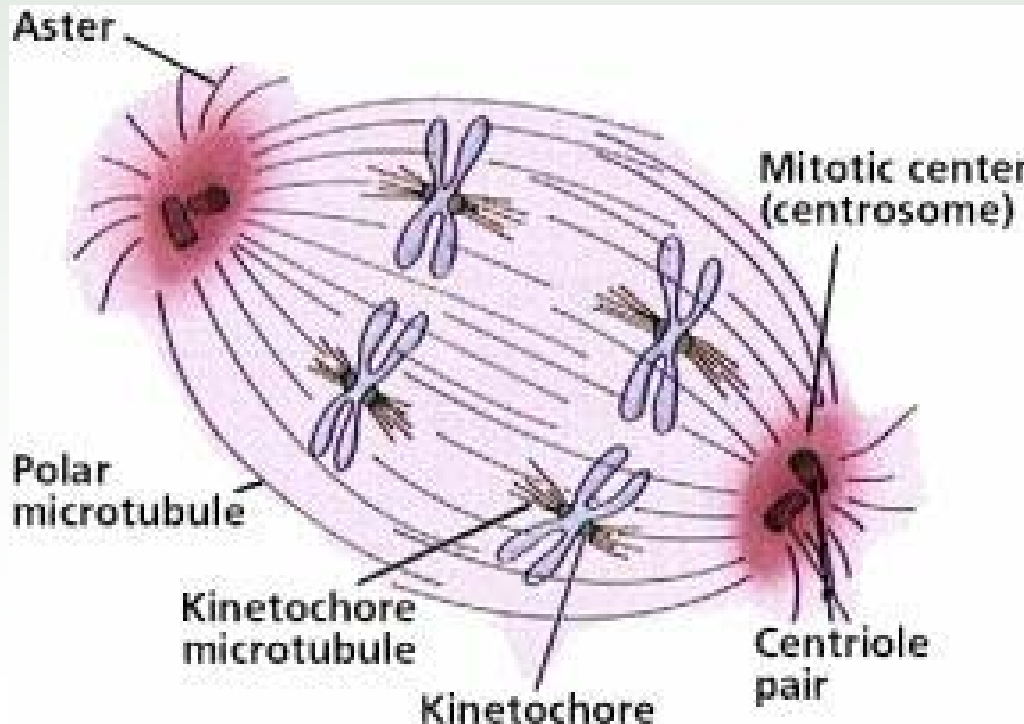


From Vale Lab, UC San Francisco

<http://valelab.ucsf.edu>

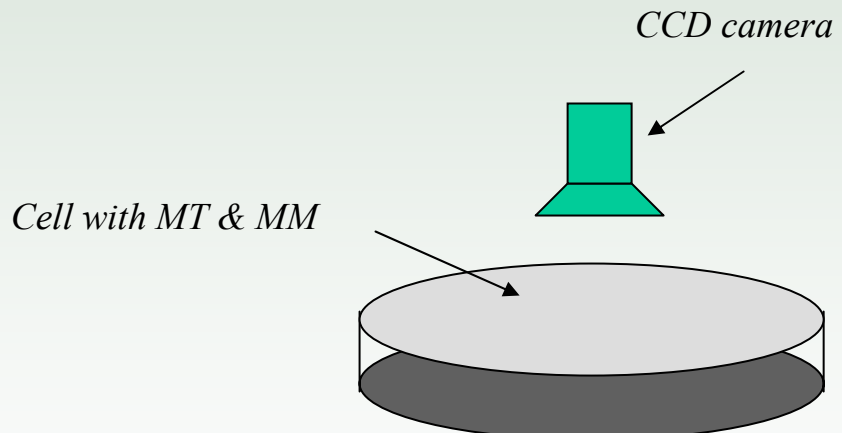
Dividing Cells and Miotic/Mitotic Spindles

- MT form cytoskeleton of dividing cells
- Separate chromosomes



in-vitro Experiments with MT and MM

- Simplified system with only few purified components
- Experiments performed in 2D glass container: diameter 100 μm , height 5 μm
- Controlled tubulin/motor concentrations and fixed temperature
- MT have fixed length 5 μm due to fixation by taxol



F. Nedelec, T. Surrey, A. Maggs, S. Leibler,

Self-Organization of Microtubules and Motors, Nature, 389 (1997)

T. Surray, F. Nedelec, S. Leibler & E. Karsenti,

Physical Properties Determining Self-Organization of Motors & Microtubules, Science, 292 (2001)

Y. Vugmeyster, E. Berliner, J. Gelles,

Release of Isolated Single Kinesin Molecules from Microtubules, Biochemistry 37, 747 (1998).

R.D. Vale, R.A. Milligan,

The way things move: looking under the hood of molecular motor proteins. Science 288, 88 (2000) 9

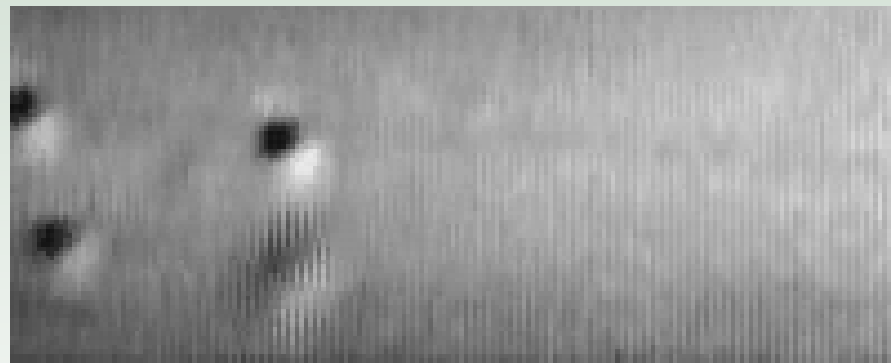
Single-molecule experiments

microtubule gliding on fixed kinesin
(R.D.Vale)



- <http://valelab.ucsf.edu>

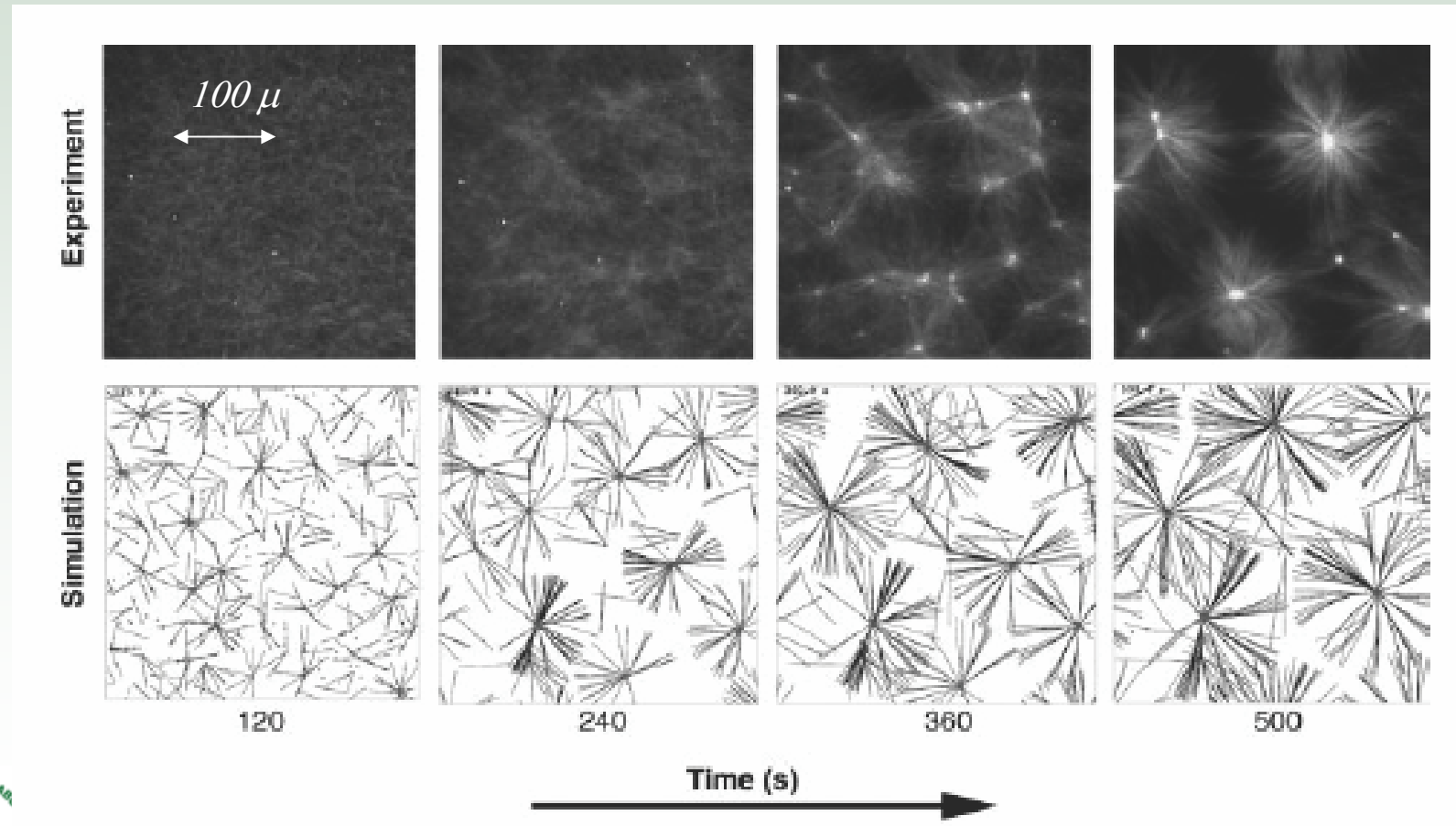
kinesin moving a bead along MT
(Vugmeyster, Berliner, Gelles (1998))



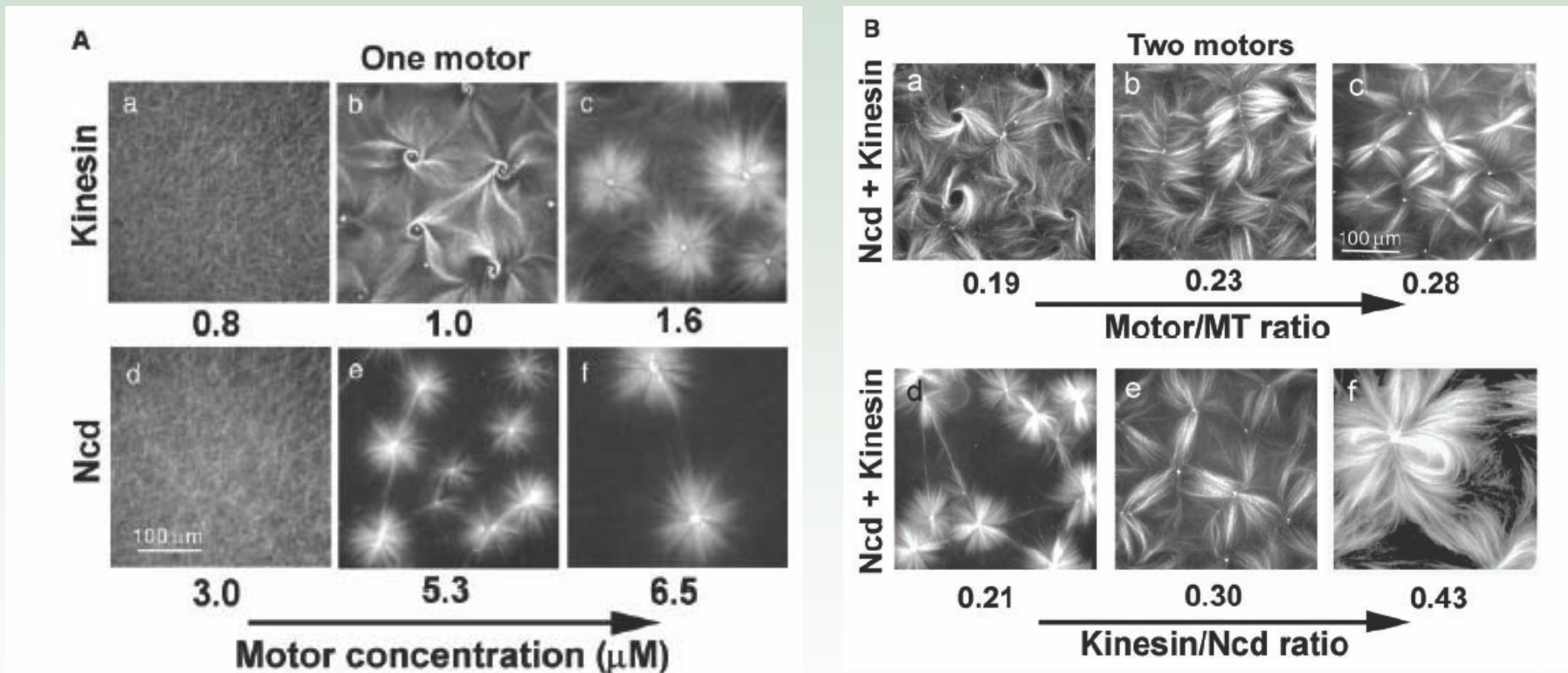
<http://www.bio.brandeis.edu/~gelles/>

Patterns in MM-MT mixtures

Formation of asters, large kinesin concentration (scale 100 μ)



Vortex – Aster Transitions



Ncd – glutathione-S-transferase-nonclaret disjunctional fusion protein
Ncd walks in opposite direction to kinesin

Dynamics of Aster/Vortex Formation

Kinesin



Ncd



Rotating Vortex

Kinesin

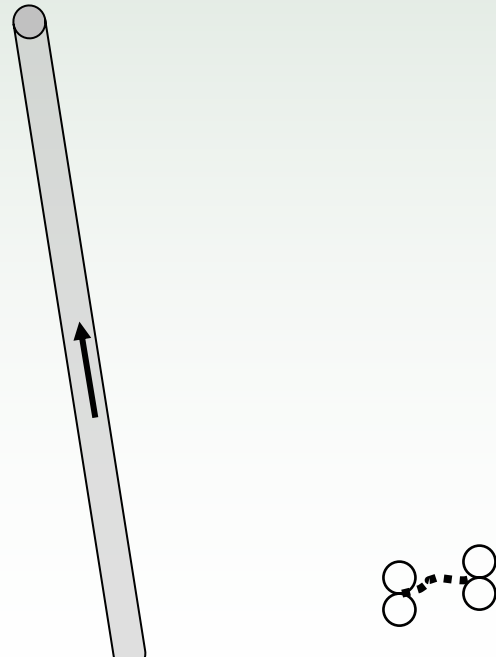


Summary of Experimental Results

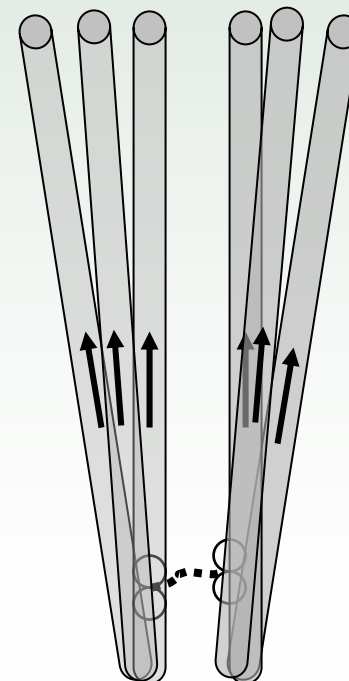
- 2D mixture of MM & MT exhibits pattern formation
- In kinesin vortices are formed for low density of MM and asters are formed for higher density
- In Ncd only asters are observed for all MM densities
- For very high MM density asters disappear and bundles formed

Mechanism of Self-Organization

Motor binding to 1 MT – no effect



*Motor binding to 2 MT – mutual orientation after interaction
Zipper effect*



Review of theoretical results

- Lee & Kardar, PRE 64 (2001) – continuum phenomenological model for MM density and motor orientation
- Kruse, Joanny, Julicher, Prost, Sekimoto, PRL 92 (2004) – general phenomenological theory for active viscoelastic gels
- Liverpool and Marchetti, PRL 90 (2003) – continuum model derived from microscopic interaction roles

Asters, Vortices, and Rotating Spirals in Active Gels of Polar Filaments

K. Kruse,¹ J. F. Joanny,² F. Jülicher,¹ J. Prost,^{2,3} and K. Sekimoto^{2,4}¹*Max-Planck Institut für Physik komplexer Systeme, Nöthnitzerstrasse 38, 01187 Dresden, Germany*²*Institut Curie, Section de Recherche, Physicochimie Curie (CNRS-UMR168), 26 rue d'Ulm 75248 Paris Cedex 05 France*³*E.S.P.C.I., 10 rue Vauquelin, 75231 Paris Cedex 05, France*⁴*LDFC Institut de Physique, 3 rue de l'Université, 67084 Strasbourg Cedex, France*

(Received 1 July 2003; published 20 February 2004)

The generalized flux-force relations for this problem read

$$2\eta u_{\alpha\beta} = \left(1 + \tau \frac{D}{Dt}\right) \times \left[\sigma_{\alpha\beta} + \zeta \Delta \mu p_\alpha p_\beta + \bar{\zeta} \Delta \mu \delta_{\alpha\beta} - \frac{\nu_1}{2} (p_\alpha h_\beta + p_\beta h_\alpha) - \bar{p}_1 p_\gamma h_\gamma \delta_{\alpha\beta} + \tau A_{\alpha\beta} \right], \quad (1)$$

$$\begin{aligned} \frac{dp_\alpha}{dt} = & - (v_\gamma \partial_\gamma) p_\alpha - \omega_{\alpha\beta} p_\beta - \nu_1 u_{\alpha\beta} p_\beta - \bar{p}_1 u_{\beta\beta} p_\alpha \\ & + \frac{1}{\gamma_1} h_\alpha + \lambda_1 p_\alpha \Delta \mu, \end{aligned} \quad (2)$$

$$r = \zeta p_\alpha p_\beta u_{\alpha\beta} + \bar{\zeta} u_{\alpha\alpha} + \lambda \Delta \mu + \lambda_1 p_\alpha h_\alpha. \quad (3)$$

Instabilities of Isotropic Solutions of Active Polar Filaments

Tanniemola B. Liverpool^{1,3} and M. Cristina Marchetti^{2,3}

¹*Applied Mathematics, University of Leeds, Leeds LS2 9JT, United Kingdom*

²*Physics Department, Syracuse University, Syracuse, New York 13244*

³*Kavli Institute of Theoretical Physics, University of California, Santa Barbara, California 93106*

The filaments are modeled as rigid rods of length l and diameter $b \ll l$. Each filament is identified by the position \mathbf{r} of its center of mass and a unit vector $\hat{\mathbf{n}}$ pointing towards the polar end. Taking into account *filament transport*, the normalized filament probability distribution function, $\Psi(\mathbf{r}, \hat{\mathbf{n}}, t)$, obeys a conservation law [13],

$$\partial_t \Psi + \nabla \cdot \mathbf{J} + \mathcal{R} \cdot \mathbf{J}' = 0, \quad (1)$$

where $\mathcal{R} = \hat{\mathbf{n}} \times \partial_{\hat{\mathbf{n}}}$ is the rotation operator. The translational and rotational currents \mathbf{J} and \mathbf{J}' are given by

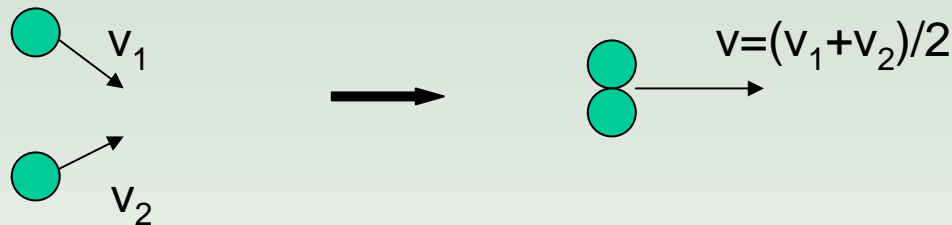
$$J_i = -D_{ij}\partial_j \Psi - \frac{D_{ij}}{k_B T} \Psi \partial_j V_{ex} + J_i^{\text{act}}, \quad (2)$$

$$\partial_t \delta \rho = \frac{1}{d} [D_{\parallel} + (d-1)D_{\perp}] (1 + v_0 \rho_0) \nabla^2 \delta \rho - \frac{\alpha l v_0 \rho_0}{12d} \nabla^2 \delta \rho - \frac{\beta l^2 v_0 \rho_0 (2d+1)}{24d(d+2)} \nabla^2 (\nabla \cdot \mathbf{t}), \quad (11)$$

$$\begin{aligned} \partial_t t_i &= -D_r t_i + \frac{1}{d+2} [(d+1)D_{\perp} + D_{\parallel}] \nabla^2 t_i + \frac{2}{d+2} (D_{\parallel} - D_{\perp}) \partial_i \nabla \cdot \mathbf{t} \\ &\quad - \frac{\alpha l v_0 \rho_0}{12d(d+2)} [\nabla^2 t_i + 2\partial_i \nabla \cdot \mathbf{t}] + \frac{\beta v_0 \rho_0}{d} \partial_i \delta \rho + \frac{\beta l^2 v_0 \rho_0 (2d+1)}{24d^2(d+2)} \partial_i \nabla^2 \delta \rho. \end{aligned} \quad (12)$$

Maxwell Model for Inelastic Particles

in-elastic grains



$$\begin{pmatrix} v_1^a \\ v_2^a \end{pmatrix} = \begin{pmatrix} \gamma & 1-\gamma \\ 1-\gamma & \gamma \end{pmatrix} \begin{pmatrix} v_1^b \\ v_2^b \end{pmatrix}$$

v^a & v^b velocities after/before collision

$\gamma=0$ – elastic collisions

$\gamma=1/2$ – fully inelastic collision

$\gamma=1$ – no interaction

Probability distributions $P(v)$

- Collision rate g does not depend on relative velocity (Maxwell molecules)
- No spatial dependence
- D - thermal diffusion, $D \sim T$, T – temperature of heat bath
- Binary uncorrelated collisions

Distribution function for $\gamma=1/2$

$$\frac{\partial P(v)}{\partial t} = D \frac{\partial^2 P(v)}{\partial v^2} + g \int_{-\infty}^{\infty} du_1 \int_{-\infty}^{\infty} du_2 P(u_1) P(u_2) [\delta(v - (u_1 + u_2)/2) - \delta(v - u_2)]$$

heat bath

source term

sink term



Results for Maxwell Model

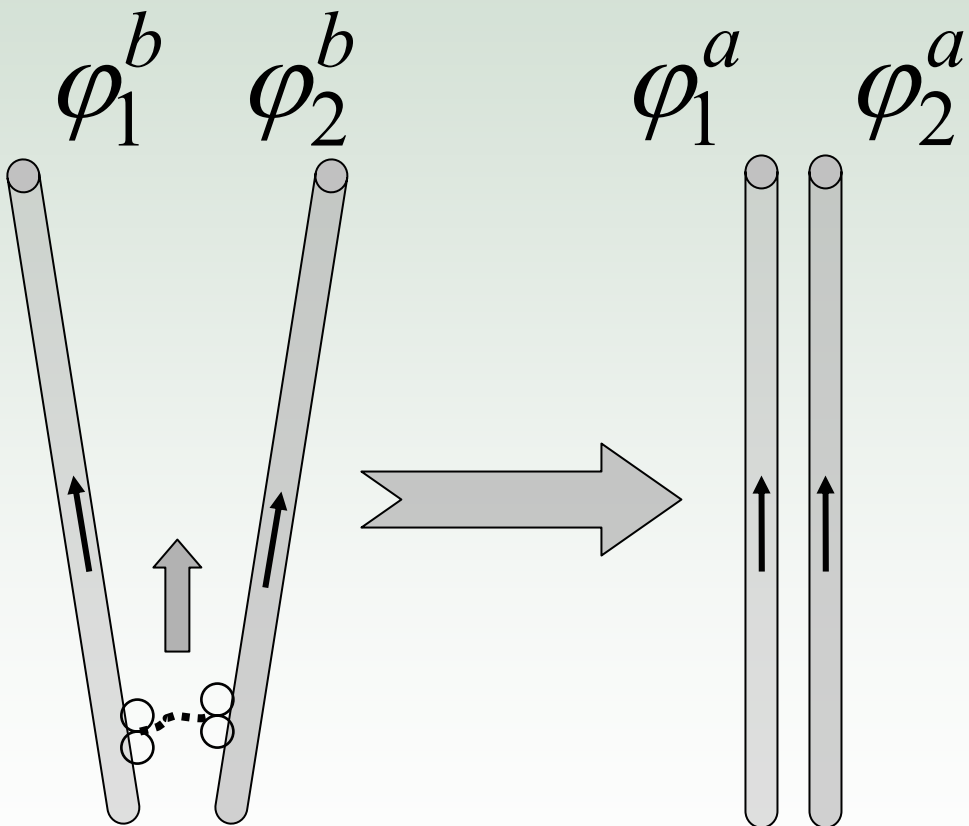
- Nice toy model: solution can be obtained analytically by the Fourier Transform of $P(v)$
- Asymptotic distribution $P(v)$ is localized but not Gaussian, the width depends on the temperature
- No phase transition, the diffusion can be scaled out

$$\text{for } \gamma = \frac{1}{2}$$

$$\frac{\partial P(v)}{\partial t} = \frac{\partial^2 P(v)}{\partial v^2} + \int_{-\infty}^{\infty} du \left[P(v + \frac{1}{2}u)P(v - \frac{1}{2}u) - P(v)P(v-u) \right]$$



Inelastic Collision of Polar Rods



$$\varphi_1^a = \varphi_2^a = \frac{1}{2}(\varphi_1^b + \varphi_2^b)$$

$\varphi_{1,2}$ – orientation angles

Fully Inelastic Collision!!!

Probability distributions $P(\varphi)$

- D_r - thermal rotational diffusion
- g – collision efficiency (\sim concentration of motors)
since diffusion of motors \gg diffusion of microtubules
assume $g=const$

$$\frac{\partial P(\varphi)}{\partial t} = D_r \frac{\partial^2 P(\varphi)}{\partial \varphi^2} + g \int_{-\pi}^{\pi} du \left[P(\varphi + \frac{1}{2}u)P(\varphi - \frac{1}{2}u) - P(\varphi)P(\varphi - u) \right]$$

- Main difference – integration over finite interval due to 2π periodicity of the angle
- There is a phase transition as g increases!!!

Stability of disoriented state

- No preferred orientation: $P(\varphi) = P_0 = 1/2\pi$
- Small perturbations: $P(\varphi) = 1/2\pi + \xi_n e^{\lambda t + in\varphi} + c.c.$
 λ – growth-rate of linear perturbations

$$\lambda_1 = g(4/\pi - 1) - D_r$$

For $g > D_r/(4/\pi - 1) \approx 3.662 D_r$ - disoriented state loses stability

Orientation phase transition above critical motor density !!!

Macroscopic Variables

- Density of MT $\rho = 2\pi \langle P(\varphi) \rangle = \int_{-\pi}^{\pi} P(\varphi) d\varphi$

- Average orientation $\tau = (\tau_x, \tau_y)$

$$\tau_x = \frac{1}{2\pi} \int_{-\pi}^{\pi} \cos \varphi P(\varphi) d\varphi \quad \tau_y = \frac{1}{2\pi} \int_{-\pi}^{\pi} \sin \varphi P(\varphi) d\varphi$$

- “Complex orientation” $\psi = \tau_x + i\tau_y = \frac{1}{2\pi} \int_{-\pi}^{\pi} e^{i\varphi} P(\varphi) d\varphi$



Fourier Expansion

$$P(\varphi) = \sum_{n=-\infty}^{\infty} P_n e^{in\varphi}; \quad P_n = \frac{1}{2\pi} \int_{-\pi}^{\pi} P(\varphi) e^{-in\varphi} d\varphi$$

Relation to observables

$$\rho = 2\pi P_0; \quad \psi = P_{-1}; \quad \psi^* = P_1$$



Asymptotic expansion for P_n ($\gamma=1/2$)

$$\dot{P}_k + (\textcolor{red}{D_r} k^2 + 1) P_k = 2\pi \sum_n \sum_m P_n P_m \frac{\sin[\pi(n-m)/2]}{\pi(n-m)/2} \delta_{n+m,k}$$

Scaling of variables $t \rightarrow D_r t;$ $P_n \rightarrow \frac{g}{D_r} P_n$

- Diffusion $-D_r k^2$ forces rapid decay higher harmonics
- Linear growth rates λ_n

$$\lambda_0 = 0$$

$$\lambda_1 = (4/\pi - 1) - D_r > 0$$

$\lambda_n < 0$ for $|n| \geq 2$ Neglect higher harmonics

Asymptotic Landau Equation

- Truncation of series for $|n| > 2$

$$\frac{\partial \rho}{\partial t} = 0$$

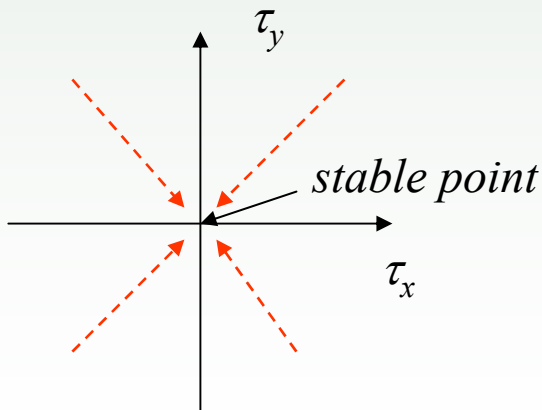
$$\frac{\partial \tau}{\partial t} = \left(\left(\frac{4}{\pi} - 1 \right) \rho - 1 \right) \tau - \frac{16\pi}{3(4 + \rho)} |\tau|^2 \tau \approx \left(0.273\rho - 1 \right) \tau - 2.18 |\tau|^2 \tau$$

- Second order phase transition for $\rho > \rho_c = 1/0.273 \approx 3.662$

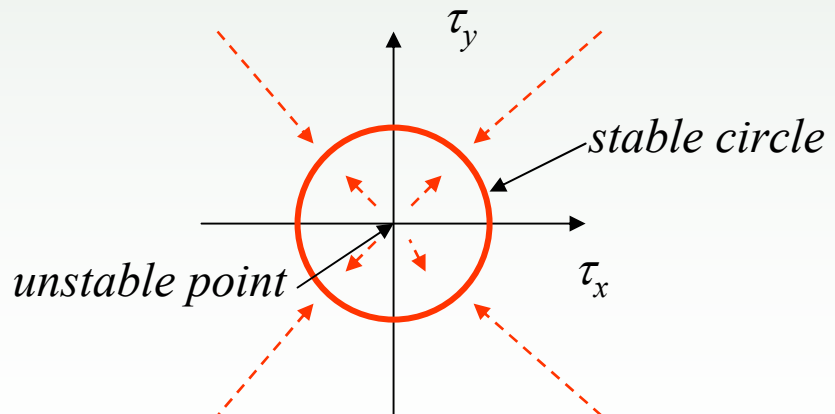
Second order phase transition for $\rho > \rho_c$

$$\frac{\partial \tau}{\partial t} \approx (\rho / \rho_c - 1) \tau - 2.18 |\tau|^2 \tau$$

$\rho < \rho_c$ – no preferred orientation
 $|\tau| \rightarrow 0$, stable point $\tau = 0$

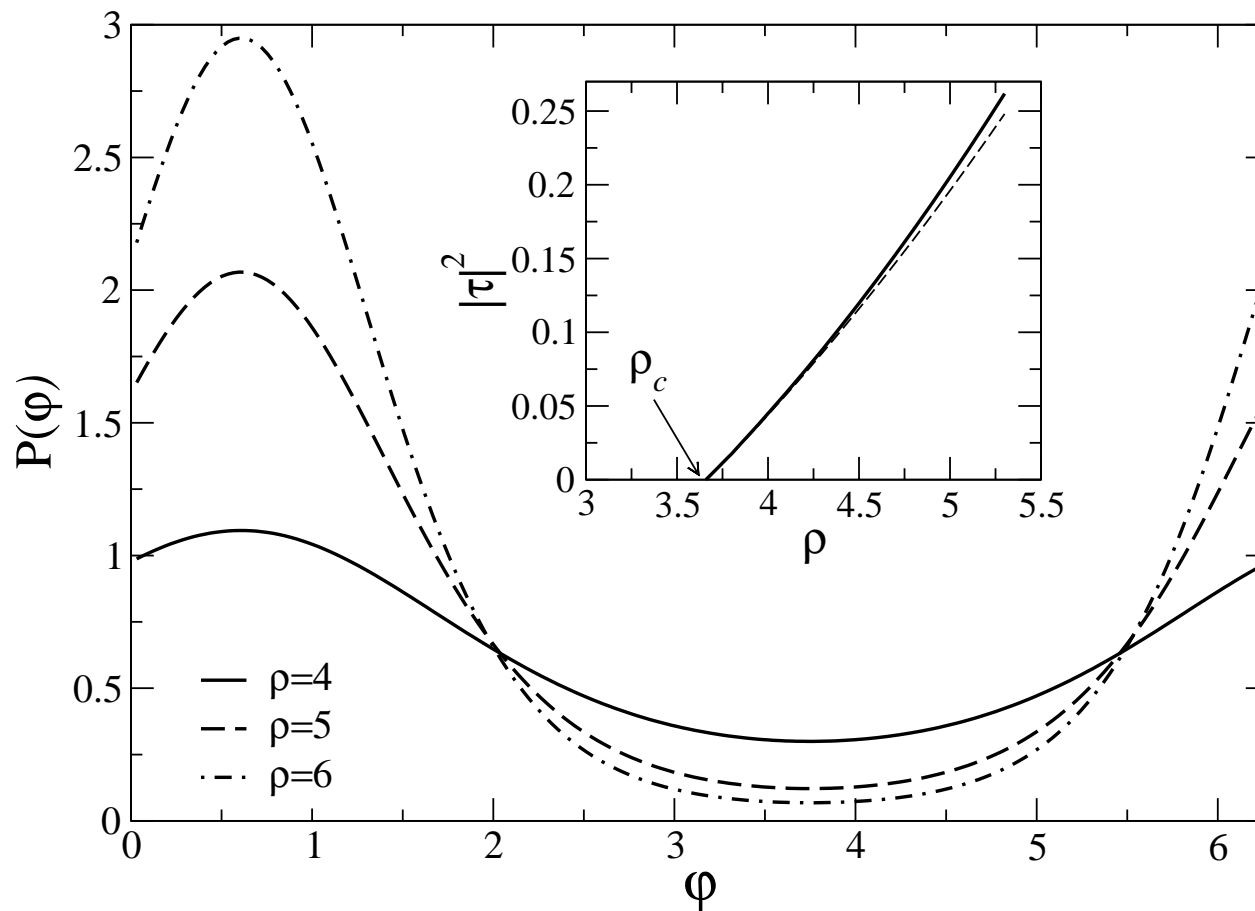


$\rho > \rho_c$ – onset of preferred orientation
 $|\tau| \rightarrow \text{const}$, direction is determined by initial distribution, stable limit circle



Compare with Hopf Bifurcation Scenario

Stationary Angular Distributions Comparison with Numerical Solution



Spatial Localization of Interaction

- Interaction between rods decay with the distance
- Translational and rotational diffusion of rods

$$\frac{\partial P(\varphi, \mathbf{r})}{\partial t} = D_r \frac{\partial^2 P(\varphi, \mathbf{r})}{\partial \varphi^2} + \partial_i D_{ij} \partial_j P(\varphi, \mathbf{r}) + g I(W : P)$$

$I(W : P)$ – collision integral

W - interaction kernel

$D_{ij} = D_{||} n_i n_j + D_{\perp} (\delta_{ij} - n_i n_j)$ – translational diffusion matrix



The Diffusion Matrix in Kirkwood Approximation

$D_{ij} = D_{\parallel} n_i n_j + D_{\perp} (\delta_{ij} - n_i n_j)$ – diffusion matrix

$\mathbf{n} = (\cos(\phi), \sin(\phi))$ – unit orientational vector

$$D_{\parallel} = k_B T \frac{\log(l/d)}{2\pi\eta_s l} \text{ – parallel diffusion}$$

$$D_{\perp} = D_{\parallel}/2 \text{ – perpendicular diffusion}$$

$$D_r = k_B T \frac{12 \log(l/d)}{\pi \eta_s l^3} \text{ – rotational diffusion}$$

l – length of the rod, d – diameter, η_s – viscosity of solvent

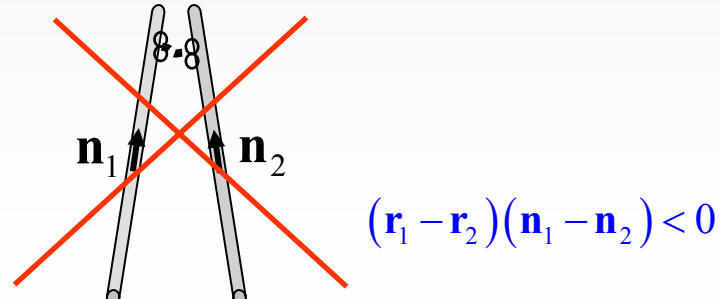
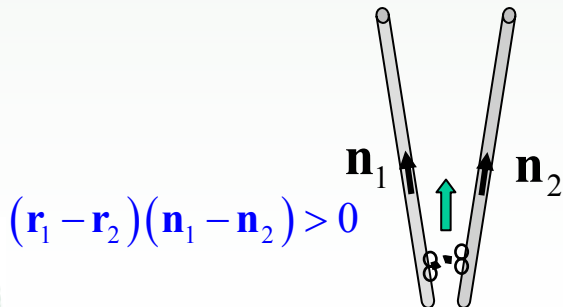
Interaction Kernel

- Decays with distance between rods
- Depends on relative angle between rods
- Symmetric with respect permutation of rods

$$W(\mathbf{r}_1, \mathbf{r}_2, \varphi_1, \varphi_2) = \frac{1}{\pi b^2} \exp\left[-\frac{|\mathbf{r}_1 - \mathbf{r}_2|^2}{b^2}\right] \left(1 + \beta (\mathbf{r}_1 - \mathbf{r}_2)(\mathbf{n}_1 - \mathbf{n}_2)\right)$$

$b = O(l)$ interaction scale

β characterizes anisotropy of interaction between polar rods



Collision Integral

$$I(W : P) = \iint d\mathbf{r}_1 d\mathbf{r}_2 \iint d\phi_1 d\phi_2 P(\phi_1, \mathbf{r}_1) P(\phi_2, \mathbf{r}_2) W(\phi_1, \mathbf{r}_1, \phi_2, \mathbf{r}_2) \times \\ \times [\delta(\mathbf{r} - (\mathbf{r}_1 + \mathbf{r}_2)/2) \delta(\phi - (\phi_1 + \phi_2)/2) - \delta(\mathbf{r} - \mathbf{r}_2) \delta(\phi - \phi_2)]$$

Continuum Equations

$$\frac{\partial \rho}{\partial t} = \nabla^2 \left[\frac{\rho}{32} - \frac{B^2 \rho^2}{16} \right] + \frac{\pi B^2 H}{16} \left[3\nabla(\boldsymbol{\tau} \nabla^2 \rho - \rho \nabla^2 \boldsymbol{\tau}) + 2\partial_i (\partial_j \rho \partial_j \tau_i - \partial_i \rho \partial_j \tau_j) \right] - \frac{7B^4 \rho_0 \nabla^4 \rho}{256}$$

$$\begin{aligned} \frac{\partial \boldsymbol{\tau}}{\partial t} = & (0.273\rho - 1)\boldsymbol{\tau} - 2.18 |\boldsymbol{\tau}|^2 \boldsymbol{\tau} + \frac{5\nabla^2 \boldsymbol{\tau}}{192} + \frac{\nabla \nabla \cdot \boldsymbol{\tau}}{96} + \frac{B^2 \rho_0 \nabla^2 \boldsymbol{\tau}}{4\pi} + \\ & + H \left[\frac{\nabla \rho^2}{16\pi} - \left(\pi - \frac{8}{3} \right) \boldsymbol{\tau} (\nabla \cdot \boldsymbol{\tau}) - \frac{8}{3} (\boldsymbol{\tau} \nabla) \boldsymbol{\tau} \right] \end{aligned}$$

$$r \rightarrow \frac{r}{l} \quad B = \frac{b}{l} \quad < 1/2 \text{ normalized cutoff length}$$

$$H = \frac{\beta b^2}{l} \quad \text{normalized kernel anisotropy}$$



Term $\partial \rho_t \sim \nabla \rho \boldsymbol{\tau} + \dots$ prohibited by the momentum conservation ³⁶

Asters and Vortices

- For $HB^2 \ll 1$ equations split and become independent

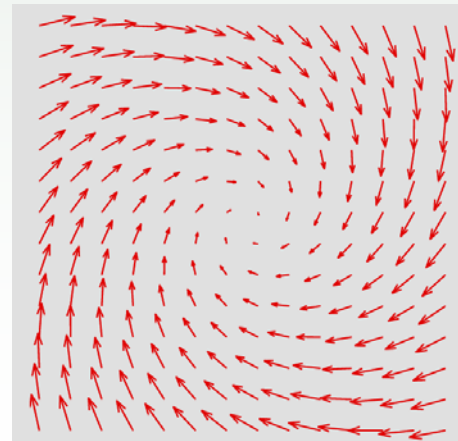
$$\frac{\partial \boldsymbol{\tau}}{\partial t} = (0.273\rho - 1)\boldsymbol{\tau} - |\boldsymbol{\tau}|^2 \boldsymbol{\tau} + \frac{5\nabla^2 \boldsymbol{\tau}}{192} + \frac{B^2 \rho_0 \nabla^2 \boldsymbol{\tau}}{4\pi} + \frac{\nabla \nabla \cdot \boldsymbol{\tau}}{96} - H [0.321\boldsymbol{\tau}(\nabla \cdot \boldsymbol{\tau}) - 1.81(\boldsymbol{\tau} \nabla) \boldsymbol{\tau}]$$

- Without blue and red terms Eq possesses “Abrikosov Vortex Solution”

$$\psi = \tau_x + i\tau_y = F(r) \exp[i\theta + i\varphi]$$

r, θ -polar coordinates

$\varphi = \text{const}$ arbitrary phase (tilt angle)

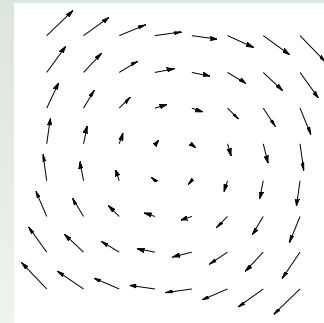


Vortices vs Aster

- For $H=0$ (**no red terms**) the only stable solutions $\phi = \pm\pi/2$

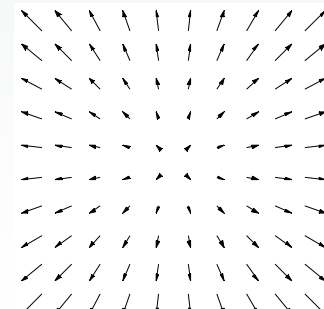
Vortex: MT tilted off the center

Aranson & Tsimring, PRE 2003

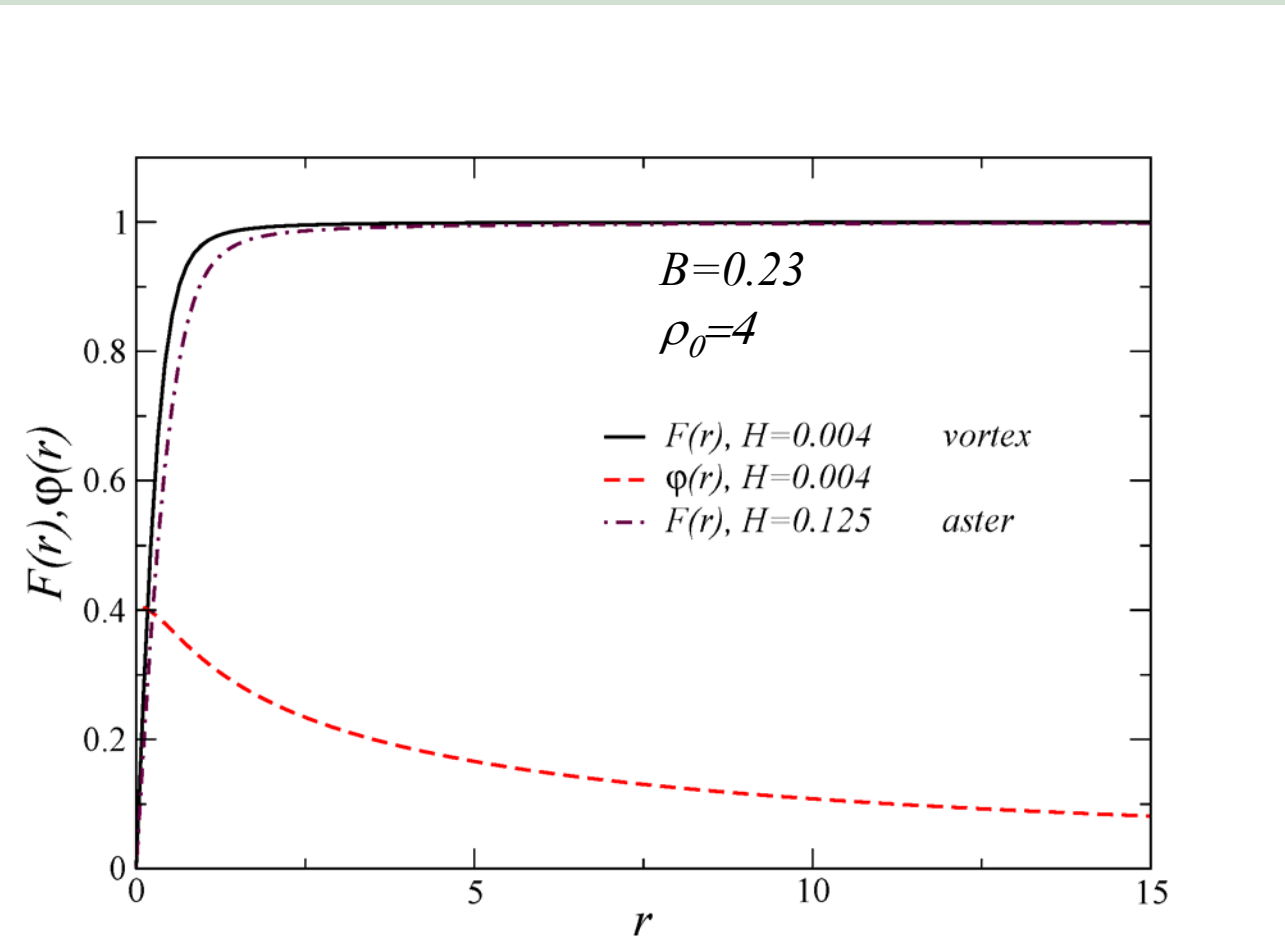


- For $H \neq 0$ (**no blue terms**) the only stable solution $\phi = 0$

Aster: MT directed towards the center



Vortex/Aster Solutions



For $H \neq 0$ far away from the core the distinction between vortex and aster disappears

Linear Instability of Aster

$$\psi = \tau_x + i\tau_y = (F(r) + we^{\lambda t}) e^{i\vartheta}$$

r, ϑ – polar coordinates

F – aster solution function

w - linear perturbation

λ - linear growth rate



Linearized Equation for Aster

$$\lambda w = (D_{\parallel} - D_{\perp}) \Delta_r w + (1 - F^2 - 0.31H\nabla_r F) w - 1.81HF\nabla_r w$$

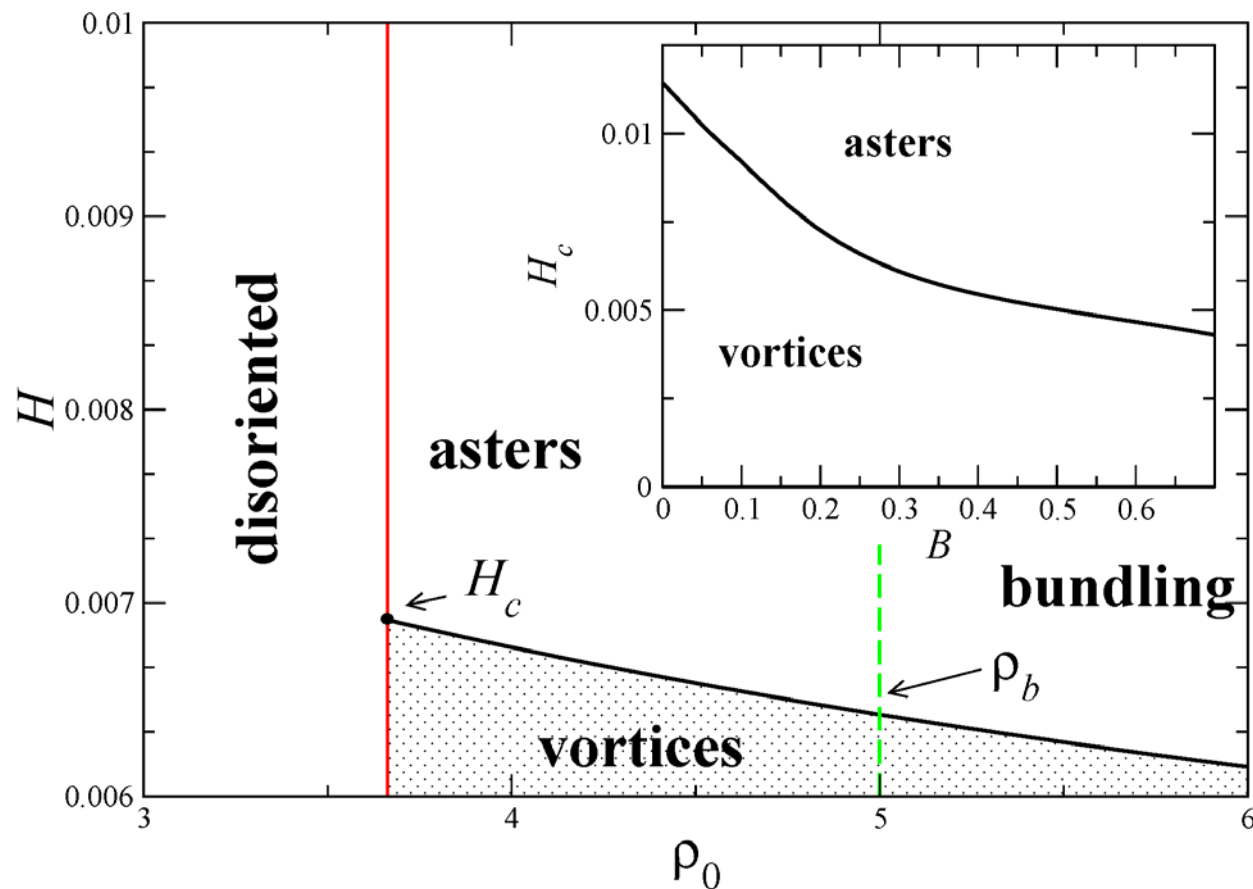
$$\Delta_r = \partial_r^2 + \cancel{\partial}_r - \cancel{1}/r^2$$

$$\nabla_r = \partial_r + \cancel{1}/r$$

*Equations solved numerically by shooting-matching
method with Newton iterations*



Phase Diagram



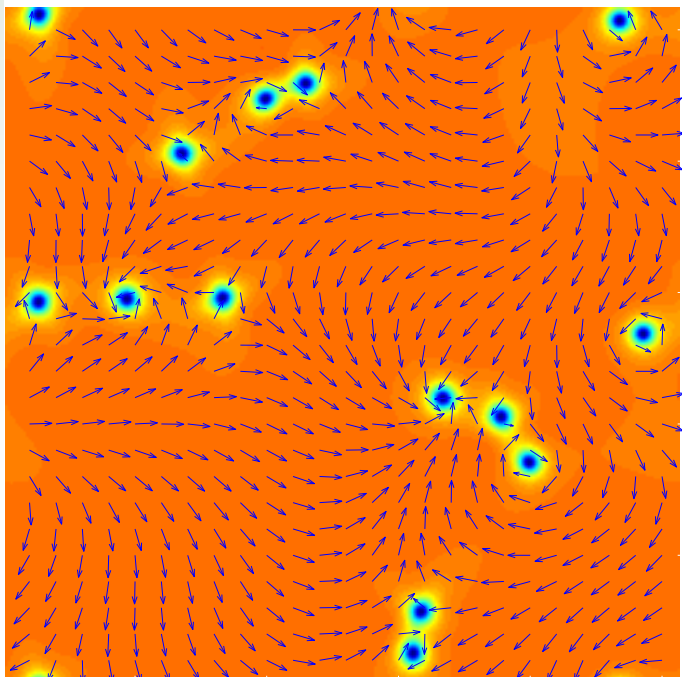
Implications of Analysis

- Aster stable for large MM density
- Vortices stable only for low MM density
- No stable vortices for $H > H_c$ for all MM density
(in experiments no vortices in Ncd for all densities)

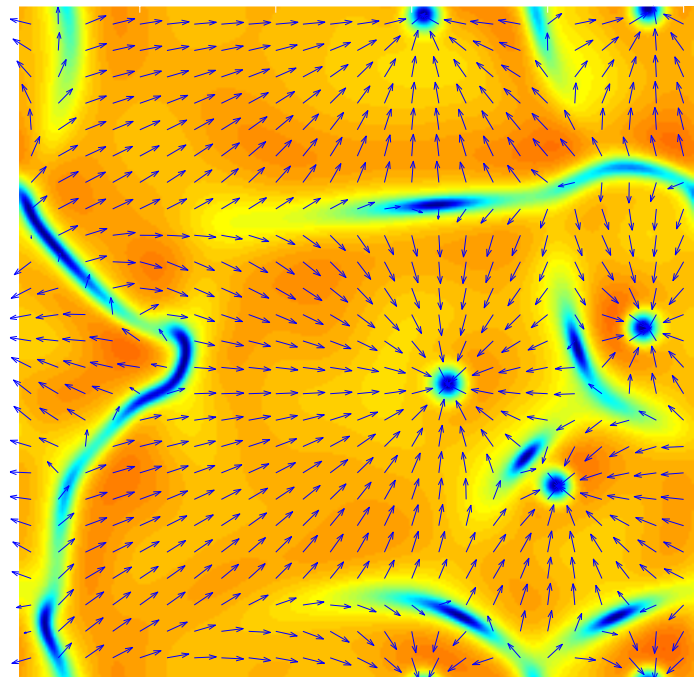
Numerical Solution

- Quasispectral Method ; 256x256 FFT harmonics
- Periodic boundary conditions
- Spontaneous creation of vortices and asters

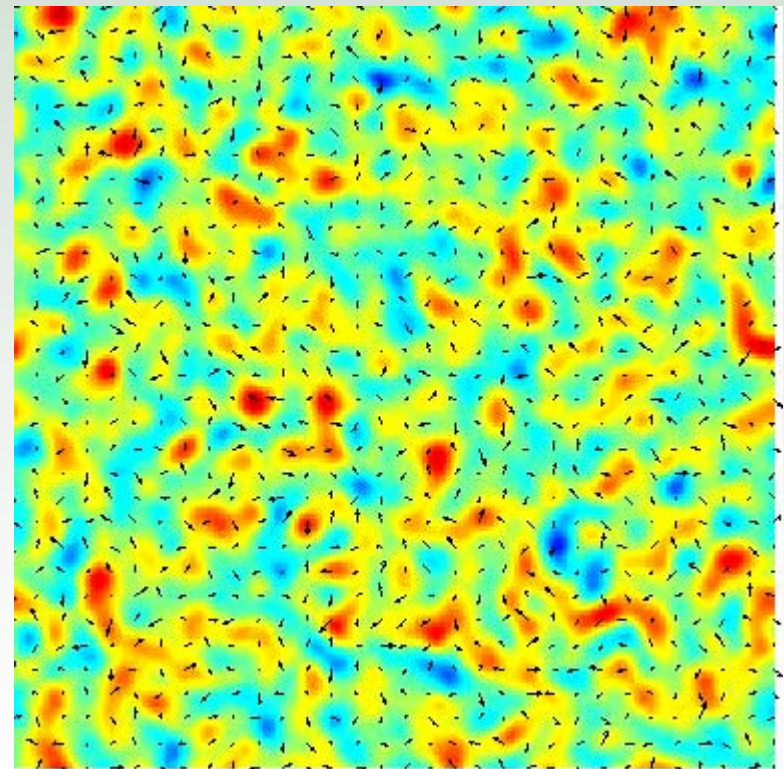
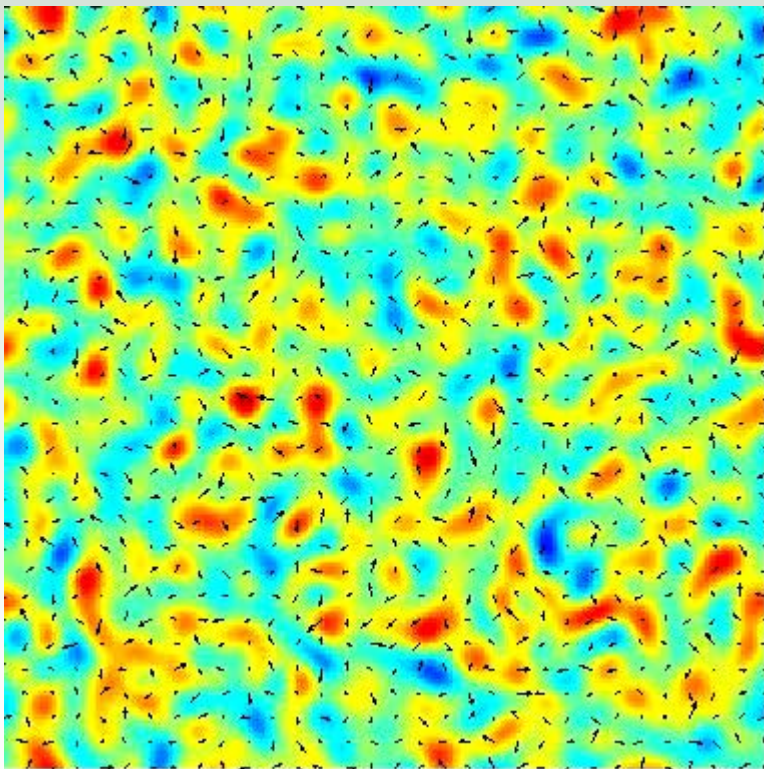
$H=0.004$



$H=0.125$



Evolution of Vortices and Aster

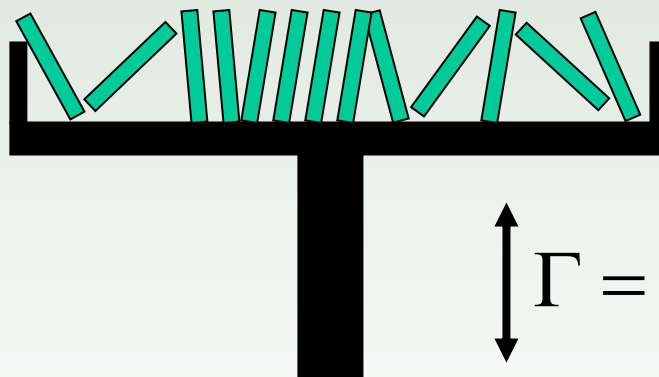


Conclusions

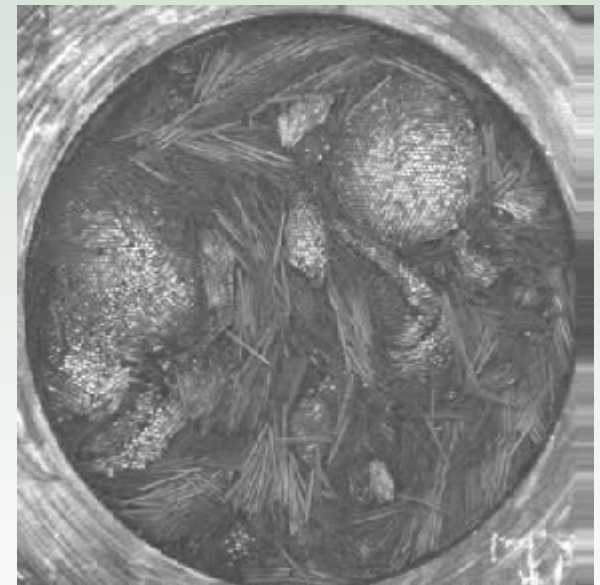
- Equations derived from microscopic model
- Reasonable agreement with experiment
- Possible applications for biological and non-biological systems:
 - biofilm formation by bacteria
 - organization of self-propelled particles (vibrated rods)

Blair-Kudrolli experiment

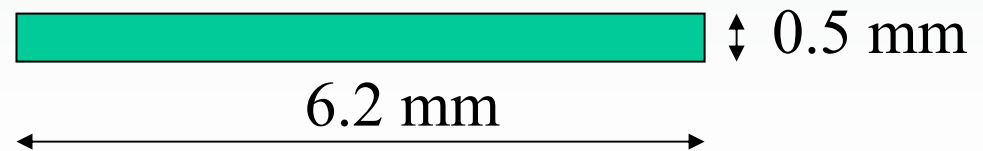
vibration of long rods



top view



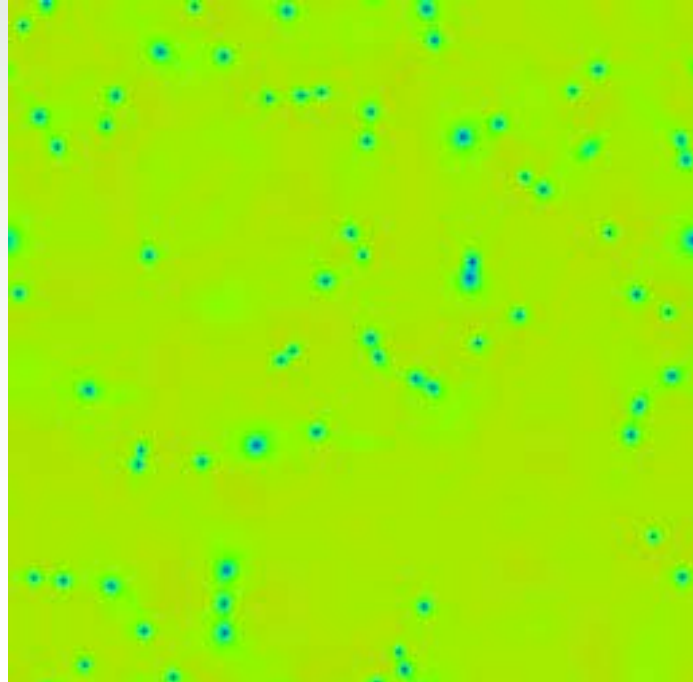
long Cu cylinders
of particles 10^4



Theoretical Description, I.A & L.T PRE (2003)

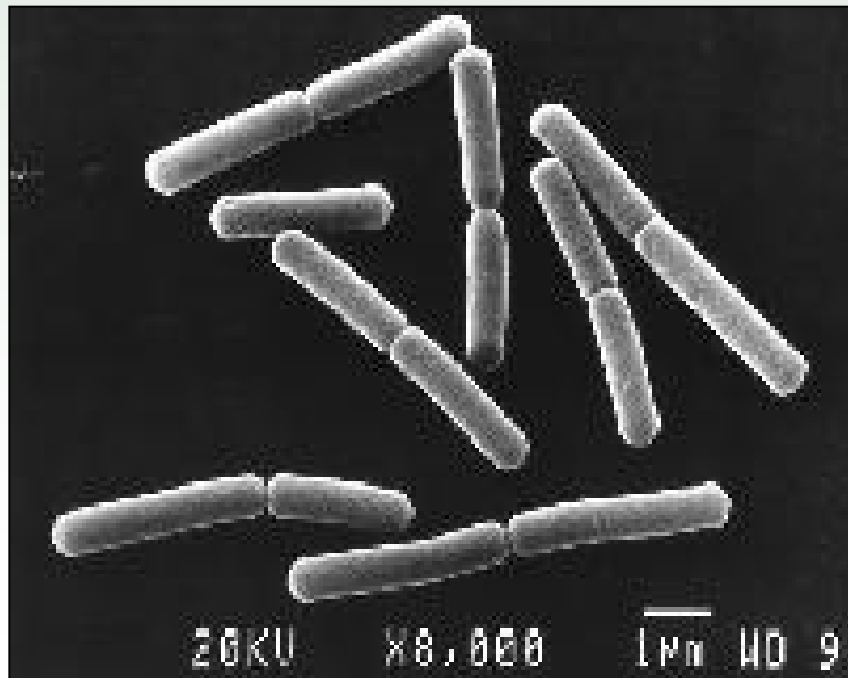
$$\partial_t \rho = -\frac{1}{\zeta} \nabla^2 \cdot (\nabla^2 \rho - \rho(1-\rho)(\delta - \rho)) + \alpha \nabla \cdot (\mathbf{n} f_0(n)(\rho + \rho_0))$$

$$\partial_t \mathbf{n} = f_1(\rho) \mathbf{n} - |\mathbf{n}|^2 \mathbf{n} + f_2(\rho) (\xi_1 \nabla^2 \mathbf{n} + \xi_2 \nabla \nabla \cdot \mathbf{n}) + \beta \nabla \rho$$



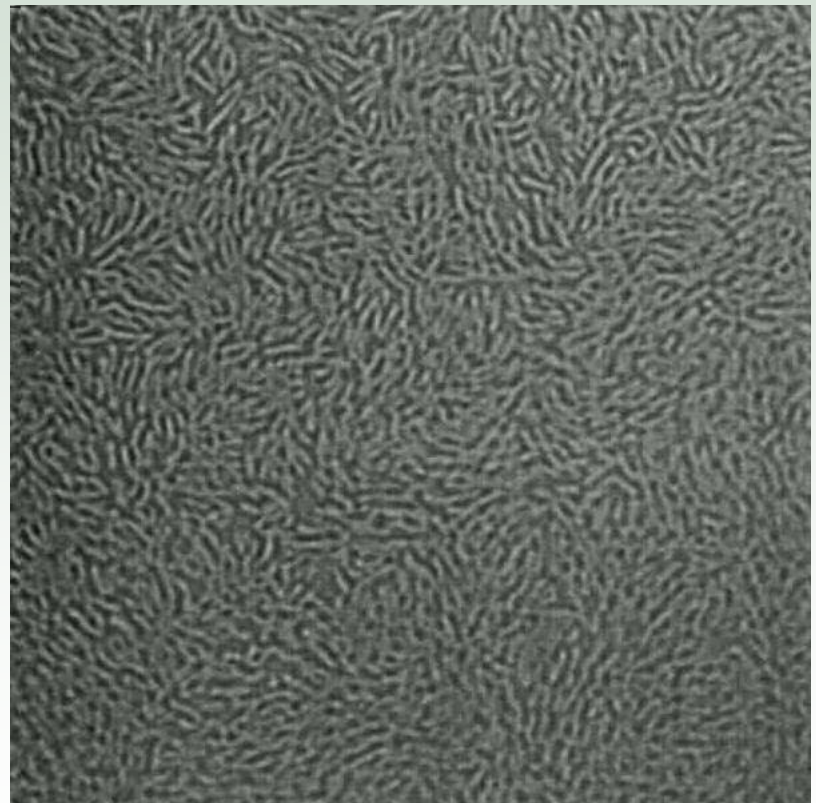
Self-propelled bioparticles

- swimming bacteriuia *Bacillus subtilis*
- length 5 μm , speed 20 $\mu\text{m/sec}$
- collective flows up to 100 $\mu\text{m/sec}$



Turbulence in bacterial monolayer

- Experiment in fluid film
(Andrey Sokolov and I.A.
Argonne), collaboration with U
Arizona (Ray Goldstein)
- Elementary interactions:
 - self-propulsion
 - hydrodynamic attraction
(aka inelastic collision)
 - flow advection
 - direction realignment in shear
flow



Theoretical model

- Ginzburg-Landau equation for orientation
- Coupled Navier-Stokes Equation for fluid velocity

